

# Neutron sources during shell C-burning in massive stars

Marco Pignatari<sup>1</sup>, R. Gallino<sup>1</sup>, C. Baldovin<sup>1</sup>  
and F. Herwig<sup>2</sup>

<sup>1</sup>Dipartimento di Fisica Generale, Via P. Giuria 1, Torino 10125, Italia  
email: pignatar@ph.unito.it, gallino@ph.unito.it, baldovin@studenti.ph.unito.it

<sup>2</sup>Los Alamos National Laboratory, Los Alamos, NM 87544, USA  
email: fherwig@lanl.gov

**Abstract.** We present a study of the s–process nucleosynthesis (weak s–process) occurring during convective core He–burning and convective shell Carbon–burning in a massive star of 25 M<sub>⊙</sub>. We use an updated nuclear network for the various neutron sources and for all neutron captures and β–decay rates involved. Large uncertainties affect the final yields due to the present unsatisfactory knowledge of all neutron capture cross sections involved.

**Keywords.** Nuclear reactions, nucleosynthesis, abundances, stars: abundances

---

During the presupernova evolution of a massive star, the convective core He–burning and the convective shell Carbon–burning phases are the astrophysical sites of the *weak* s–process, the region between iron and  $A \simeq 90$ . During core He burning, we use the same stellar evolutionary model as in Raiteri *et al.* (1991a). The  $^{22}\text{Ne}(\alpha, n)^{25}\text{Mg}$  reaction by Jaeger *et al.* (2001) is the major neutron source. The neutron capture network has been updated, using the Bao *et al.* (2000) recommended cross sections for radiative neutron captures, and a number of recent (n,p) and (n,α) channels. During core He burning the most important neutron poisons are the primary  $^{16}\text{O}$  and the metallicity-dependent  $^{25}\text{Mg}$ . As a test, the shell C–burning nucleosynthesis is followed with a post–processing code, as in Raiteri *et al.* (1991b), using a constant temperature  $T = 1.05 \times 10^9$  K and a density  $\rho = 10^5$  cm<sup>−3</sup>. The network is extended up to all unstable isotopes along the s–path with a β<sup>−</sup> half–life down to 5 minutes. During C burning, α particles and protons are made available by the direct channels  $^{12}\text{C}(^{12}\text{C}, \alpha)^{20}\text{Ne}$  and  $^{12}\text{C}(^{12}\text{C}, p)^{23}\text{Na}$ . The neutron density reaches a peak value of  $3 \times 10^{11}$  cm<sup>−3</sup> in the initial phase and then decreases following the decrease of α–particles. As shown in Fig. 1a, the most important neutron source is  $^{13}\text{C}(\alpha, n)^{16}\text{O}$ , where primary  $^{13}\text{C}$  results from  $^{12}\text{C}(p, \gamma)^{13}\text{N}(\beta^+)^{13}\text{C}$ . A primary abundance of  $^{17}\text{O}$  is synthesised by the  $^{16}\text{O}(n, \gamma)^{17}\text{O}$  channel. It gives rise to another important neutron source via the reaction  $^{17}\text{O}(\alpha, n)^{20}\text{Ne}$  (Caughlan & Fowler 1988). However a strong competing reaction is  $^{17}\text{O}(n, \alpha)^{14}\text{C}$  (Schatz *et al.* 1993). As shown in Fig. 1b,  $^{16}\text{O}$  is the most important neutron poison during the initial phase of shell C–burning, followed by  $^{25}\text{Mg}$  and  $^{17}\text{O}$ . In Fig. 2a the final production factors  $X_i/(X_i)_\odot$  in the shell C–burning region are compared with the production factors at the end of core He–burning. The strong contribution to the final weak s–process yields by shell C–burning is evident, in particular in the Kr–Rb–Sr region. The final yields suffer from a large uncertainty in the Kr–Rb–Sr region close to neutron magic  $N = 50$ . This is due to the quite large uncertainty (up to 20%) of all the neutron capture cross sections involved, including the light neutron poisons. In Fig. 2b we show that increasing by 20% the neutron capture cross sections of all stable isotopes between  $^{57}\text{Fe}$  and  $^{82}\text{Se}$ , the final production factors in the region Kr–Rb–Sr change by a factor of

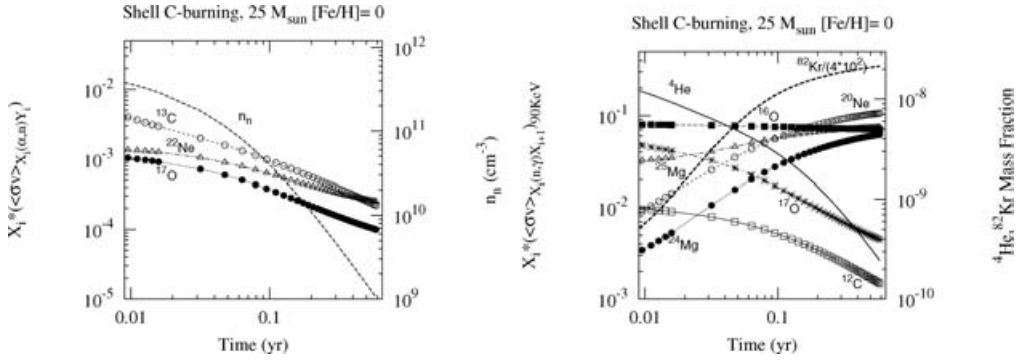


**Figure 1.** Panel a): Temporal behaviour during shell C–burning of the neutron density and of the mass fractions of the major neutron sources multiplied by their  ${}^iX(\alpha,n)^iY$  rates (90 KeV). Panel b): Temporal behaviour during shell C–burning of the most important neutron poisons multiplied by their respective neutron capture cross sections at 90 KeV. Plotted are also the mass fractions of  ${}^4\text{He}$  and  ${}^{82}\text{Kr}\cdot 10^2$ .

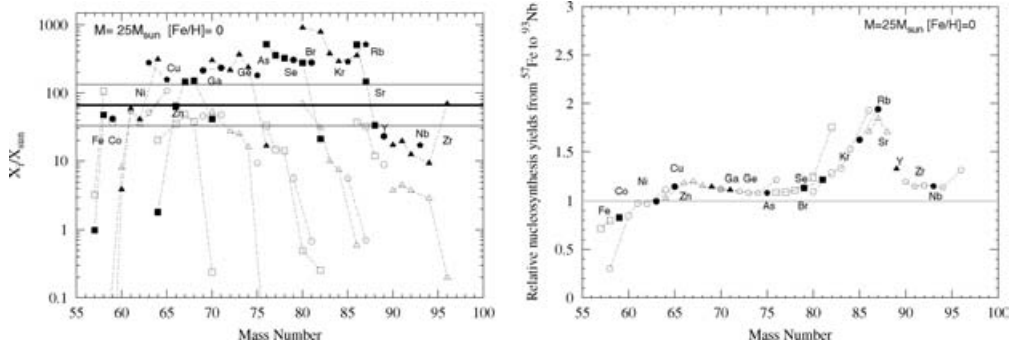


**Figure 2.** Panel a): Production factors between  ${}^{57}\text{Fe}$  and  ${}^{93}\text{Nb}$  at the end of core He–burning (empty symbols) and at the end of shell C–burning (full symbols). Panel b): Ratio with respect to the standard case of the final yields after shell C–burning in a test case where all neutron capture cross sections between  ${}^{57}\text{Fe}$  and  ${}^{82}\text{Se}$  have been increased by 20%.

1.5–2. To conclude, during the shell C–burning the most important neutron source is primary  ${}^{13}\text{C}(\alpha,n){}^{16}\text{O}$  and the most important neutron poison is primary  ${}^{16}\text{O}(n,\gamma){}^{17}\text{O}$ . This implies a secondary-like behaviour of the weak s–process with varying the initial metallicity.

**References**

Bao, Z.Y., Beer, H., Käppeler, F., Voss, F., Wisshak, K., & Rauscher, T. 2000, *ADNDT* 76, 70  
 Caughlan, G.R. & Fowler, W.A. 1988, *ADNDT* 40, 283  
 Jaeger, M., *et al.* 2001, *Phys. Rev. Lett.* 87, 2501  
 Raiteri, C.M., Busso, M., Gallino, R., Picchio, G., & Pulone, L. 1991, *ApJ* 367, 228  
 Raiteri, C.M., Busso, M., Picchio, G., & Gallino, R. 1991, *ApJ* 371, 665  
 Schatz, H., Käppeler, F., Koehler, P.E., Wiescher, M., & Trautvetter, H.-P. 1993, *ApJ* 413, 750